Science of the Total Environment 647 (2019) 895–904

Contents lists available at ScienceDirect

Science of the Total Environment

journal homepage: www.elsevier.com/locate/scitotenv

Net ecosystem carbon and greenhouse gas budgets in fiber and cereal cropping systems

Chunyan Liu [a,*], Zhisheng Yao [a], Kai Wang [a], Xunhua Zheng [a,b], Baoguo Li [c]

[a] State Key Laboratory of Atmospheric Boundary Layer Physics and Atmospheric Chemistry (LAPC), Institute of Atmospheric Physics, Chinese Academy of Sciences, Beijing 100029, China
[b] University of Chinese Academy of Sciences, Beijing 100049, China
[c] Department of Soil and Water Sciences, China Agricultural University, Beijing 100094, China

HIGHLIGHTS

- Net ecosystem carbon and greenhouse gas budgets are evaluated for two years.
- Cotton cropping system functions as a large carbon (C) and greenhouse (GHG) source.
- Wheat-maize copping system is a C and GHG sink in the years without wind damage.
- Net C sequestration higher in double cropping systems than single cropping systems.
- Traditional rotation between double and single cropping systems should be restored.

GRAPHICAL ABSTRACT

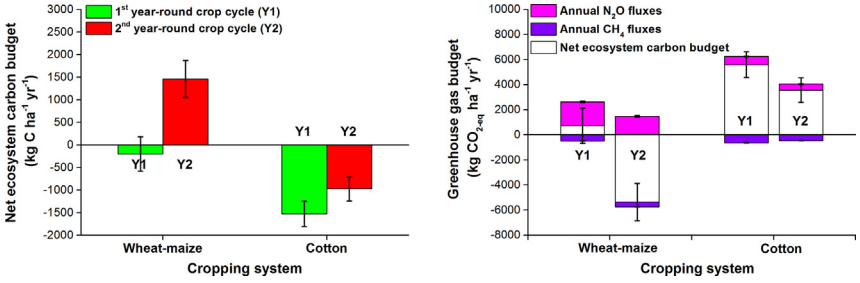

ARTICLE INFO

Article history:
Received 19 June 2018
Received in revised form 1 August 2018
Accepted 4 August 2018
Available online 5 August 2018

Editor: Jay Gan

Keywords:
Net ecosystem exchange
Net ecosystem production
Methane
Nitrous oxide
Extreme weather
Rotational cropping system

ABSTRACT

To assess the contributions of fiber and cereal production on climate change, the net ecosystem exchange of carbon dioxide (CO_2), main exchanges of non-CO_2 carbon, and methane (CH_4) and nitrous oxide (N_2O) fluxes were continuously monitored throughout two year-round crop cycles (Y1 and Y2: 1st and 2nd year-round crop cycles, respectively) using eddy covariance, biometric observation, and static chamber methods in typical cotton and wheat–maize rotational cropping systems in China. The evaluation of net ecosystem carbon budgets (NECBs: considering net ecosystem CO_2 exchange and non-CO_2 carbon exchanges by fertilization, seeding, and harvest) and greenhouse gas budgets (GHGBs: adding CH_4 and N_2O fluxes to the NECBs based on CO_2 equivalents) showed that the cotton cropping system persistently functioned as an intensive carbon (−1527 and −974 kg C ha^{-1} yr^{-1}) and greenhouse gas (GHG) source (5618 and 3591 kg CO_2-eq ha^{-1} yr^{-1}) because of the large CO_2 emissions during the long fallow periods (5748 and 5160 kg CO_2 ha^{-1} in Y1 and Y2, respectively). The wheat–maize cropping system had high net ecosystem production (NEP) and low harvest index and therefore, served as a notable carbon sink (1461 kg C ha^{-1} yr^{-1} in Y2). Although high irrigation water and chemical fertilizer inputs stimulated N_2O emissions, the wheat–maize cropping system still behaved as an important GHG sink (−4257 kg CO_2-eq ha^{-1} yr^{-1} in Y2) because of the tremendous net carbon sequestration. However, in Y1 incidental wind damage lowered the NEP and turned the wheat–maize cropping system into a GHG source (2144 kg CO_2-eq ha^{-1} yr^{-1}). The NEP, NECBs, and GHGBs of the double cropping system generally exceeded those of the single cropping system. The traditional rotation between double and single cropping systems should be restored to maintain soil carbon storage and alleviate the radiative forcing effects of cotton production.

© 2018 Elsevier B.V. All rights reserved.

* Corresponding author.
E-mail address: lcy@post.iap.ac.cn (C. Liu).

https://doi.org/10.1016/j.scitotenv.2018.08.048
0048-9697/© 2018 Elsevier B.V. All rights reserved.

1. Introduction

Although agricultural expansion and intensification have successfully increased the production of fiber, cereal, biofuel, and other products to sustain human life, these processes have also substantially intensified climate change (Foley et al., 2011). Agroecosystems influence climate through variations of ecosystem carbon storage and exchanges of greenhouse gases (GHGs), such as methane (CH_4) and nitrous oxide (N_2O), between the biosphere and atmosphere. The net carbon accumulation (positive) or loss rates (negative value) in an ecosystem can be defined as net ecosystem carbon budgets or balances (NECBs, Chapin et al., 2006). The NECBs at the annual scale can be quantified by an integrated measurement of the net ecosystem exchange of carbon dioxide (CO_2) and exchanges of non-CO_2 carbon (Smith et al., 2010). The integrated measurement provides a good solution for evaluating the short-term (year by year) effects of management practices and extreme weather on the NECBs. Recently, efforts have been made to quantify the NECBs of food and cash crops by eddy covariance integrated with biometric observation methods (Aubinet et al., 2009; Béziat et al., 2009; Ceschia et al., 2010; Kutsch et al., 2010; Bhattacharyya et al., 2013). Because of the diversity in management practices, soil types and climate, the experimental croplands can be net carbon neutral, sources, or sinks, which indicates the complicated effects of agricultural production on climate change.

Besides the effects on the NECBs, agricultural production also exerts diverse effects on the biosphere–atmosphere exchanges of GHGs. For instance, the extensive applications of organic and inorganic fertilizers greatly increase N_2O emissions and soil organic carbon (SOC) storage but have various effects (positive, negative, or none) on CH_4 uptake in upland croplands (Liu et al., 2011, 2012, 2014). A complete understanding of the role of agricultural production on climate change requires an integrated assessment of NECBs, and CH_4 and N_2O exchanges. Very few studies have conducted the evaluation of greenhouse gas budgets or balances (GHGBs), which are calculated by adding CH_4 and N_2O fluxes to the NECBs based on the concepts of CO_2 equivalents (CO_2-eq). Ceschia et al. (2010) evaluated the effects of cropping systems, extreme weather, and management practices on the GHGBs in representative European croplands based on eddy covariance, biometric observation, emission factors, and literature review methods. A few studies also assessed the long-term averaged effects of management practices on the GHGBs based on the measurements of SOC density variations (typically over years to decades) and CH_4 and N_2O fluxes (Robertson et al., 2000; Shang et al., 2011; Huang et al., 2013; Zhang et al., 2016).

Cotton, wheat, and maize are the most important fiber and cereal crops. However, studies on the GHG fluxes, NECBs, and GHGBs in cotton cropping systems are scarce worldwide (Scheer et al., 2008; Liu et al., 2010; Lv et al., 2014). China is a major producer of cotton, wheat, and maize, accounting for approximately 1/5 to 1/4 of the global production (China Statistical Yearbook, 2017). The production of wheat and maize is greatly dependent on the one-year winter wheat–summer maize rotational cropping system, which is widely distributed on the North China Plain and Fen-wei Plain in China. The double cropping systems are major N_2O sources (0.8–6.9 kg N ha^{-1} yr^{-1}) due to excessive irrigation (90–690 mm yr^{-1}) and fertilization (550–600 kg N ha^{-1} yr^{-1}) (Liu et al., 2014). However, the integrated climate effects, as characterized by the NECBs and GHGBs, remain undetermined in the double cropping systems.

To quantify the contributions of cotton, wheat, and maize production to climate change, the main components of NECBs and CH_4 and N_2O fluxes were detected over two year-round crop cycles in a typical cotton cropping system and winter wheat–summer maize rotational cropping system in the Fen-wei Plain, which is one of the seven major agricultural regions in China. The cotton and winter wheat–summer maize rotational cropping systems are widespread on the plain. The aims of this study were to quantify the NECBs and GHGBs of typical cotton and wheat–maize rotational cropping systems and evaluate the roles of cotton, wheat, and maize production on climate change.

2. Materials and methods

2.1. Site descriptions

Two adjacent cotton (200 × 100 m, 34°55.50′N, 110°42.59′E) and wheat–maize rotational (220 × 100 m, 34°55.51′N, 110°42.59′E) fields were studied, situated within the Dong Cun Farm in Yuncheng City, Shanxi province, China. Maize (*Zea mays* L.) grows between early June and mid-October (row spacing: 60 cm, plant spacing: 25 cm), and wheat (*Triticum aestivum* L.) grows during the remainder of the year (row spacing: 20 cm). Cotton is sown with plastic mulch in early April at a density of 5.5–5.9 plants m^{-2}. Inter-tillage (0–5 cm) is applied 2–3 times per year between April and June for weeding and root development in the cotton field. Seed cotton (cotton lint and seed) is manually harvested once every 1–2 weeks between the end of August and early November. The cotton field then remains in bare fallow until early April of the following year. After harvest, all crop residues are mechanically chopped into pieces (5–10 cm length) and ploughed into the soil (0–20 and 0–40 cm for the wheat–maize and cotton fields, respectively). Pesticides are applied weekly to the cotton field from mid-May to mid-August and only once during July in the wheat–maize field. Herbicides are applied once (at the end of March) and twice (in early March and at the end of June) in the cotton and wheat–maize fields, respectively. These crops are irrigated with deep groundwater (bore hole depth: 130–140 m) by a sprinkler system. Nitrogen (N), phosphorus (P), and potassium (K) fertilizers in the form of urea, calcium superphosphate, and potassium sulfate are applied once to twice (sowing and the flowering and boll-setting stage of cotton) and three times per year (sowing, the greening stage of wheat, and the 18- to 19-leaf stage of maize) in the cotton and wheat–maize fields, respectively. The fertilizer is either tilled into the soil (0–20 cm) after surface broadcasting at seeding time or covered by the soil (0–5 cm) after band application along the plant row. Modern management practices (such as plastic mulch culture, crop residue amendment, and sprinkler irrigation) gradually replaced traditional practices (field burning of crop residue and flood irrigation) on this farm after 2000. The cotton and wheat–maize fields have been planted with these crops since April 2004 and October 2005, respectively. The two cropping systems were rotated every 2–3 years before 2004 in both fields. More detailed management information, soil properties, and meteorological data are provided in Table 1.

2.2. Calculations of NECBs and GHGBs

The NECBs in croplands equal the total carbon inputs (C_{inputs}: photosynthesis, seeding, fertilization, and deposition) minus the total carbon exports ($C_{exports}$: respiration, non-respiration CO_2 emissions, non-CO_2 carbon gas emissions, harvest, pests, erosion, and eluviation). The eddy covariance net ecosystem exchange (NEE) represents the overall CO_2 balance of photosynthesis (gross primary productivity), respiration (plant and soil respiration), and non-respiration processes (fire, ultraviolet oxidation of organic matter, and atmosphere–water equilibration). Since fire is seriously prohibited in the present fields, the CO_2 exchanges of non-respiration processes are minor terms of CO_2 exchanges and can be ignored. Therefore, net ecosystem production (NEP: the difference of gross primary production and ecosystem respiration) is approximately equal to cumulative NEE but has the opposite sign. The NEP and main non-CO_2 carbon exchanges (fertilization, seeding, and harvest) were measured to estimate the NECBs (unit: kg C ha^{-1} $season^{-1}$ or yr^{-1}). The other minor non-CO_2 carbon exchanges were either absent (herbivory) or ignored (pest, erosion, eluviation, volatile organic compounds, carbon monoxide, and methane exchanges) in the present estimation of NECBs. The GHGBs were calculated by adding CH_4 and N_2O fluxes to the NECBs based on the $CO_{2\text{-eq}}$ (unit: kg CO_2-eq ha^{-1} $season^{-1}$ or yr^{-1}). The system boundaries of the estimated GHGBs were defined to the field scale. The carbon emissions from agrichemical production

Table 1
Soil properties, meteorological data, and management information for the wheat–maize and cotton fields.

	Unit	Wheat–maize		Cotton	
Organic carbon	(g kg^{-1}, 0–10 cm)	11.3 (1.1)		10.5 (0.9)	
Total nitrogen	(g kg^{-1}, 0–10 cm)	1.12 (0.10)		1.01 (0.08)	
Water-soluble salts	(g kg^{-1}, 0–10 cm)	0.98 (0.12)		0.78 (0.05)	
pH	(0–10 cm)	8.7 (0.1)		8.6 (0.1)	
Clay (< 0.002 mm)	(%, 0–10 cm)	31.8 (1.6)		34.8 (0.8)	
Silt (0.002–0.02 mm)	(%, 0–10 cm)	38.9 (1.0)		38.9 (0.8)	
Sand (0.02–2 mm)	(%, 0–10 cm)	29.3 (2.5)		26.3 (0.5)	
Bulk density	(g cm^{-3}, 0–6 cm)	1.17 (0.07)		1.26 (0.06)	
Year-round crop cycle		Y1	Y2	Y1	Y2
Start date		15/10/2008	18/10/2009	06/11/2008	08/11/2009
End date		17/10/2009	17/10/2010	07/11/2009	05/11/2010
Period	(days)	368	365	365	363
Mean air temperature	(°C)	14.3	13.8	14.3	13.8
Mean soil temperature	(°C, 5 cm)	14.1	13.4	14.8	14.4
Mean PAR	(μmol photons m^{-2} s^{-1})	284	285	284	285
Total precipitation	(mm yr^{-1})	609	637	592	620
Amount of irrigation	(mm yr^{-1})	434	408	181	144
Mean WFPS	(%, 0–6 cm)	33.6	39.1	33.3	38.4
Mean groundwater depth	(m)	1.1	1.0	1.1	1.0
Fertilization rate	(kg N-P-K ha^{-1} yr^{-1})	390-60-30	430-60-30	75-9-10	89-30-29

Y1 and Y2: 1st and 2nd year-round crop cycles, respectively. PAR: photosynthesis active radiation. WFPS: water-filled pore space. Values in parentheses indicate standard deviations of three to six spatial replicates.

(fertilizer, pesticide, herbicide, and plastic mulch), machinery operations (fuel and electricity for tillage and irrigation), and manufacturing of agricultural machinery were not considered in the present GHGBs. The positive and negative values of GHGBs, NEE, and CH_4 and N_2O fluxes represent GHG emissions (from croplands to the atmosphere) and uptake (from the atmosphere to croplands), respectively. The positive and negative values of NECBs and NEP represent the net carbon accumulation and loss in croplands, respectively. The NECBs and NEP are opposite in sign to the GHGBs, NEE, and CH_4 and N_2O fluxes. Therefore, the NECBs and GHGBs were calculated as follows:

$$\mathrm{NEP} \approx -\mathrm{NEE}_{\mathrm{cum}}$$

$$\mathrm{NECBs} = C_{\mathrm{inputs}} - C_{\mathrm{exports}} = (\mathrm{NEP} + F_{\mathrm{seed}} + F_{\mathrm{fert}}) - F_{\mathrm{harv}}$$

$$\mathrm{GHGBs} = -\mathrm{NECBs} \times \mathrm{CO}_{2-\mathrm{eq}-\mathrm{C}} + F_{\mathrm{CH4}} \times \mathrm{CO}_{2-\mathrm{eq}-\mathrm{CH4}} + F_{\mathrm{N2O}} \times \mathrm{CO}_{2-\mathrm{eq}-\mathrm{N2O}}$$

where NEP is the net ecosystem production (kg C ha^{-1} $season^{-1}$ or yr^{-1}); NEE_{cum} stands for the cumulative NEE measured by eddy covariance method (kg C ha^{-1} $season^{-1}$ or yr^{-1}); F_{seed}, F_{fert}, and F_{harv} represent the non-CO_2 carbon exchanges by seeding, fertilization, and harvest (unit: kg C ha^{-1} $season^{-1}$ or yr^{-1}), respectively; and F_{CH4} and F_{N2O} indicate the cumulative CH_4 and N_2O fluxes measured by static opaque chamber method (kg CH_4 and N_2O ha^{-1} $season^{-1}$ or yr^{-1}), respectively. The sustained-flux global warming potential (SGWP, for gas emissions) and the sustained-flux global cooling potential (SGCP, for gas uptake) are similar to the global warming potentials (GWPs) in that they are metrics for comparing the time-integrated radiative forcing of different GHGs. However, the SGWP and SGCP are more appropriate than the GWPs when GHG fluxes persist over time rather than occur as a single pulse. Furthermore, the SGCP can better characterize the cooling effects when ecosystems uptake GHGs from the atmosphere. Thus, the concepts of SGWP and SGCP rather than GWPs are applied in the estimations of GHGBs in the present study. The SGWP value of N_2O is 270 when fluxes are leaving ecosystems (emission: positive fluxes), and the SGCP value of CH_4 is 203 when fluxes are entering ecosystems (uptake: negative fluxes), with a 100-year time horizon (Neubauer and Megonigal, 2015). The molar mass ratio of CO_2 to carbon is approximately 3.7 (44/12 ≈ 3.7). Therefore, $CO_{2\text{-eq-C}}$, $CO_{2\text{-eq-CH4}}$ and $CO_{2\text{-eq-N2O}}$ were 3.7 kg CO_2-eq kg^{-1} C, 203 kg CO_2-eq kg^{-1} CH_4, and 270 kg CO_2-eq kg^{-1} N_2O, respectively.

2.3. Field measurements

Field measurements were continuously performed over two year-round crop cycles in the cotton and wheat–maize fields (hereinafter Y1 and Y2 representing the 1st and 2nd year-round crop cycles, respectively, see Table 1). The amendment dates of maize and cotton residues were regarded as the demarcation points of the two year-round crop cycles.

2.3.1. NEE

The NEE of the wheat–maize field was measured by an eddy covariance system mainly consisting of an open-path infrared gas analyzer (LI-7500, LI-COR Inc., USA), a three-dimensional sonic anemometer (CSAT-3, Campbell Scientific Inc., USA), and a data logger (CR5000, Campbell Scientific, Inc., USA) from October 15, 2008 to October 17, 2010. The NEE of the cotton field was observed with another measuring system with the same instrumentation as mentioned above from November 6, 2008 to November 5, 2010, except the use of a different sonic anemometer (USA-1, METEK GmbH, Germany) from January 1 to December 31 of 2009. The CO_2 concentrations and wind velocity data were recorded at a frequency of 10 Hz. The gas analyzers and sonic anemometers were mounted at heights of 1.6–3.9 m (> 2 times canopy height), depending on the crop heights. The gas analyzers were slightly tilted (vertical angle 30–45°) to minimize the accumulation of rainwater on the optical windows. The gas and sonic sensors were positioned at the same height and were separated by a horizontal distance of 15–30 cm. The prevalent wind directions were from the east (60–120°) and west (240–300°). Thus, gas analyzers were placed south of the sonic anemometers to minimize their disturbance on wind velocity observations. Eddy covariance systems were placed in the middle of each field (east–west direction: 200 and 220 m for cotton and wheat–maize fields) to optimize fetch in the main wind directions. The gas analyzers were calibrated over an interval of half a year.

The NEE fluxes were calculated as the covariance of CO_2 concentrations and vertical wind velocities over a time interval of 30 min. The open-source software EddyPro (LI-COR Biosciences, 2017) was used for processing the 10 Hz raw data and flux calculation. Prior to the covariance calculation, the raw data processing included the spike removal and the replacement of spikes with linear interpolation (Vickers and Mahrt, 1997), the sonic anemometer tilt correction by the double rotation method (Wilczak et al., 2001), and the time lags

compensation by the covariance maximization method (Fan et al., 1990). The raw fluxes were corrected for the density fluctuations (Webb et al., 1980) and the spectral losses (Moncrieff et al., 1997, 2004). The surface heating effects of LI-7500 were corrected using the estimated heating correction technique (Burba et al., 2008). The instrument surface temperature was estimated via linear regression with ambient air temperature using the empirical fitting parameters in Burba et al. (2008). Then, the flux data was quality controlled using the following steps. First, flux data during precipitation, sprinkler irrigation, and instrument maintenance periods were removed. Second, stability and integral turbulence characteristic tests (Foken and Wichura, 1996; Göckede et al., 2006) were performed. The flux data with quality flags from 7 to 9 indicated unsteady and poor developed turbulent conditions and were therefore rejected. Finally, the fluxes were deleted when the footprints of interest were < 80% of the potential contribution area according to a footprint analysis (Kljun et al., 2004). Approximately 37% of the raw flux data were deleted after the quality control. To estimate the daily (unit: g CO_2 m^{-2} d^{-1}) and annual cumulative NEE (kg CO_2 ha^{-1} yr^{-1}), the half-hour fluxes were modeled for gap-filling, using the empirical Arrhenius and rectangular hyperbola equations of temperature and photosynthesis active radiation (PAR, Wang et al., 2013).

2.3.2. CH_4 and N_2O Fluxes

The CH_4 and N_2O fluxes were measured using a static, opaque chamber–gas chromatography method. The gas chromatograph configuration, design specifications of opaque chambers, and nonlinear flux calculation method (5 gas samples) are described in Wang et al. (2010) and Liu et al. (2012). The base collars (20 cm into the soil, 6 spatial replicates per site) were positioned in the plant rows and inter-rows to ensure the representativeness of the fluxes. Rubber sealing was used for the joints of the chamber and base collar to ensure the gas-tightness during the chamber closure. The ventilation tube was installed and the sample volume was minimized (10 ml for each gas sample) to relieve the effects of chamber closure and gas sampling on air pressure inside the chamber. Five gas samples of each spatial replicate were manually sampled during the chamber closure (10–40 min) at intervals of 2.5–10 min. Samples were collected daily for two weeks after fertilization and irrigation and twice per week during the remaining periods. All chamber fluxes were measured between 08:00 and 10:00 when the hourly air temperatures were close to the daily means and therefore, the average fluxes of six spatial replicates for each field were used to represent daily mean fluxes (Liu et al., 2013). The daily CH_4 and N_2O fluxes were calculated as the product of daily mean fluxes and 24 h d^{-1}, which were further aggregated to seasonal or annual totals by interpolating the arithmetic mean of the two closest sampling dates as the average flux of those days between sampling dates.

2.3.3. Yield, aboveground biomass and crop carbon content

Biomass samples were collected in four spatial replicates (sampling area: 12.0, 24.4, and 14.4 m^2 for wheat, maize, and cotton). All seed cotton, wheat and maize grains, and 1/8 of the other aboveground parts were weighed after oven drying to estimate yields and aboveground biomass. The aboveground dry matter was divided into 3 to 4 parts (grain, straw, leaf, and corncob), and the carbon content of each part was measured using the potassium dichromate method.

2.3.4. Auxiliary measurements

Air and soil (5 cm) temperatures (HMP155 and QMT 110, VAISALA, Finland), precipitation (resolution: 0.2 mm, DZZ3, Shanghai Changwang Meteotech Co., Ltd., China) and PAR (LI-190, LI-COR, Inc., USA) were continuously recorded by a meteorological station in the middle of the two fields. The amounts of sprinkler irrigation were measured by manual rain gauges. The topsoil (0–6 cm) volumetric water contents were measured daily using the oven-drying method when the soil was frozen in January, and a portable moisture probe when the soil was not frozen (ML2x, ThetaKit, Delta-T Devices, Cambridge, UK). The volumetric water contents were converted into water-filled pore space (WFPS) by using the determined bulk density and an average density of mineral soils (2.65 g cm^{-3}). The groundwater depth was measured weekly using four polyvinyl chloride tubes (length: 3 m; diameter: 6 cm) that were vertically inserted into the soil.

2.4. Uncertainty and statistical analysis

The sampling errors of eddy covariance measurement were primarily caused by the limited number of independent samples and were considered in the uncertainty analysis of half-hourly NEE fluxes. The random uncertainty of each half-hourly eddy covariance flux ($u_{\text{hh-EC}}$) was estimated based on the variance of covariance between vertical wind velocities and CO_2 concentrations (Finkelstein and Sims, 2001).

$$u_{\text{hh-EC}} = \sqrt{\frac{1}{n}\left[\sum_{p=-m}^{m}\hat{\gamma}_{w,w}(p)\hat{\gamma}_{c,c}(p) + \sum_{p=-m}^{m}\hat{\gamma}_{w,c}(p)\hat{\gamma}_{c,w}(p)\right]}$$

where $u_{\text{hh-EC}}$ represents the random uncertainty of half-hourly eddy covariance fluxes; w and c indicate the vertical wind velocity and CO_2 concentration, respectively; $\hat{\gamma}_{w,w}$ and $\hat{\gamma}_{c,c}$ are the variances of w and c, respectively; $\hat{\gamma}_{w,c}$ and $\hat{\gamma}_{c,w}$ are the covariance between w and c; n is the number of samples in the 30-min averaging time (i.e., $n = 18{,}000$ for 10 Hz data); and m is a number of samples sufficiently large to capture the integral timescale (i.e., $m = 200$ for 20 s).

The uncertainty of each gap-filled half-hour NEE flux ($u_{\text{gf-hh}}$) was estimated using the standard errors of parameter estimates in the Arrhenius and rectangular hyperbola equations for gap-filling. The uncertainty of each daily eddy covariance flux ($u_{\text{d-EC}}$) was calculated using the error propagation of $u_{\text{hh-EC}}$ and $u_{\text{gf-hh}}$ as follows:

$$u_{\text{d-EC}} = \sqrt{\sum_{i=1}^{48-n}\left[(u_{\text{hh-EC}})_i\right]^2 + \sum_{j=1}^{n}\left[(u_{\text{gf-hh}})_j\right]^2}$$

where n is a number of missing half-hour fluxes in each day.

The uncertainty of annual eddy covariance flux ($u_{\text{a-EC}}$) was calculated using the error propagation of $u_{\text{d-EC}}$ as follows:

$$u_{\text{a-EC}} = \sqrt{\sum_{i=1}^{365}\left[(u_{\text{d-EC}})_i\right]^2}$$

The uncertainty of hourly chamber flux ($u_{\text{h-Cham}}$) was mainly attributed to the instrumental noise and spatial variation. The uncertainties related to the two issues were assumed to be equal to the detection limit of the measuring system (u_{DL}) and the standard deviation of chamber fluxes measured in the six spatial replicates (u_{SD}), respectively. The detection limits of the opaque chamber-gas chromatography measuring system were 5 μg N_2O m^{-2} h^{-1} and 10 μg CH_4 m^{-2} h^{-1} when the chamber height was 50 cm, the chamber closure time was 40 min, and the gas chromatography precisions were 2 and 10 ppbv for N_2O and CH_4.

$$u_{\text{h-Cham}} = \sqrt{(u_{\text{DL}})^2 + (u_{\text{SD}})^2}$$

The daily chamber fluxes were calculated as the product of daily mean fluxes and 24 h d^{-1} and therefore, the uncertainty of daily chamber flux ($u_{\text{d-Cham}}$) was calculated as follows:

$$u_{\text{d-Cham}} = 24 \cdot u_{\text{h-Cham}}$$

The uncertainty of annual chamber flux ($u_{\text{a-Cham}}$) was calculated using the law of error propagation by considering the $u_{\text{d-Cham}}$ and the

uncertainty of gap filling for the missing daily fluxes between the sampling intervals ($u_{gf\text{-}d}$).

$$u_{a-Cham} = \sqrt{\sum_{i=1}^{365-N}\left[(u_{d-Cham})_i\right]^2 + \sum_{j=1}^{N}\left[(u_{gf-d})_j\right]^2}$$

where N is the number of missing daily CH_4 and N_2O fluxes; $u_{gf\text{-}d}$ was characterized by the standard deviation of the chamber fluxes that were used to fill the gaps.

The uncertainties related to crop yields, aboveground biomass, and crop carbon contents, and seeding and fertilization rates were mainly derived from the spatial variations, which were revealed by the standard deviations of four spatial replicates. Finally, the uncertainties of NECBs and GHGBs were assessed by combining the uncertainties related to eddy covariance and chamber fluxes, crop yields, and seeding and fertilization rates following the law of error propagation.

Nonparametric tests of two related samples (air and soil temperatures) and two independent samples (grain yield, amount of crop residue, harvest index, and crop carbon content) were applied to analyze the significance of the differences. Simple nonlinear regression was used to characterize the correlations between environmental factors (soil temperatures and WFPS) and chamber fluxes (CH_4 and N_2O), and the significance was determined using an F-test. All statistical analyses were performed using SPSS Statistics Client 19.0 (SPSS China, Beijing, China) and Origin 8.0 (OriginLab Ltd., Guangzhou, China).

3. Results

3.1. Meteorological, soil and crop information

The total precipitation in the 1st year-round crop cycle (Y1; 592 and 609 mm yr^{-1} for the cotton and wheat–maize fields, respectively) was slightly lower than that in the 2nd year-round crop cycle (Y2; 620 and 637 mm yr^{-1}, Fig. 1). The average air temperatures were 14.3 and 13.8 °C in Y1 and Y2, respectively, with maximum and minimum monthly means of 27.3 to 27.4 °C in July and −2.6 to −0.6 °C in January and December. The daily mean PAR varied between 18 and 678 μmol photons m^{-2} s^{-1}, with similar annual means in Y1 and Y2. The annual mean soil temperatures were slightly lower than the air temperatures in the wheat–maize field but higher than the air temperatures in the cotton field ($p < 0.01$). Over 55% of the annual precipitation occurred during the maize seasons, whereas 62%–70% of the irrigation water was concentrated on the wheat seasons in the wheat–maize field. Irrigation increased the WFPS up to a maximum of 67% and 69% in the cotton and wheat–maize fields, respectively. The mean WFPS and groundwater depth were generally higher in Y2 ($p < 0.01$), with more abundant rainfall than in Y1. The total water inputs from rainfall plus irrigation were similar in both year-round crop cycles (Table 1).

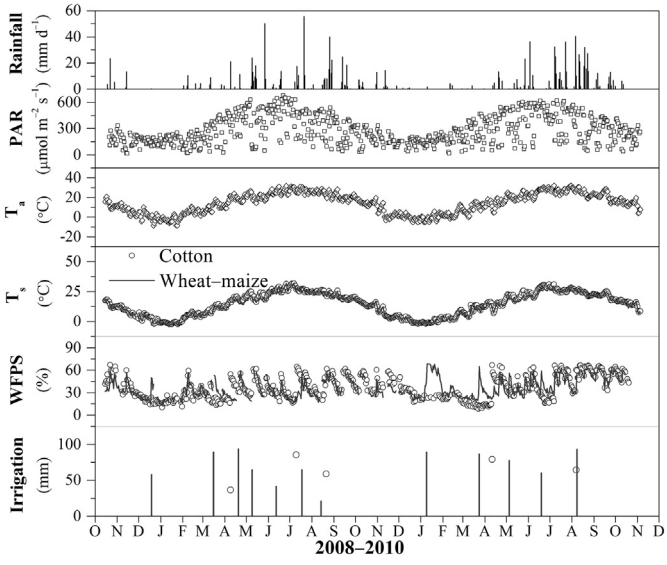

Fig. 1. Temporal variation in daily precipitation, photosynthesis active radiation (PAR), air (T_a) and soil temperatures (T_s, 5 cm), soil water-filled pore space (WFPS, 0–6 cm), and irrigation amount in the cotton and wheat–maize fields.

The amounts of seeding grains were constant in the two year-round crop cycles (Table 2). No significant differences were detected in the crop yields between the two year-round crop cycles, whereas the grain carbon contents were significantly lower in Y1 than in Y2 ($p < 0.01$). The amounts of crop residues for maize and cotton in Y1 were 34% and 25% lower ($p < 0.01$) than in Y2 because of the maize lodging and low fertilization rates in Y1. Therefore, the harvest indexes (ratios of grain yields to aboveground biomass) of maize and cotton in Y1 were significantly higher than those in Y2 ($p < 0.01$). The partial factor productivity of applied nitrogen (PFP_N: ratio of crop yield to amount of applied nitrogen) tended to be higher in the cotton field (49 ± 7 and 38 ± 5 kg seed cotton kg^{-1} N in Y1 and Y2, respectively) than in the wheat–maize field (31 ± 5 and 31 ± 6 kg grain kg^{-1} N in Y1 and Y2, respectively) because of the very low fertilization rates in the cotton field (75 and 89 kg N ha^{-1} yr^{-1} in Y1 and Y2, respectively) compared with the wheat–maize field (390 and 430 kg N ha^{-1} yr^{-1} in Y1 and Y2, respectively).

3.2. NECBs

The daily NEE in the wheat–maize field (−64.5 to 27.3 g CO_2 m^{-2} d^{-1}) showed more drastic seasonal fluctuations than that in the cotton field (−34.4 to 15.6 g CO_2 m^{-2} d^{-1}, Fig. 2). During the vigorous growth stages of wheat (March–May), maize (early July–mid-October), and cotton (mid-June–October), the fields frequently assimilated atmospheric CO_2. During the remaining periods and cloudy and rainy days, the fields emitted CO_2 to the atmosphere. Net CO_2 assimilation (negative values of daily NEE) was observed for 118 and 156 days in Y1 and 129 and 190 days in Y2 in the cotton and wheat–maize fields, respectively. The wheat–maize field presented stronger and longer net CO_2 assimilation than the cotton field. The durations of net CO_2 assimilation in Y1 were shorter than those in Y2 in both fields. The wheat–maize field switched from a CO_2 sink to a source approximately one month earlier in Y1 than in Y2 (early September vs. mid-October), because the wind damage on July 9, 2009 caused maize lodging (the bending over of the stems near the ground level as a result of the combined effects of delicate stems and extreme weather) and damaged the maize plants.

The NEP during the wheat seasons was similar in Y1 (2557 ± 36 kg C ha^{-1}) and Y2 (2381 ± 39 kg C ha^{-1}). The NEP during the maize season in Y1 (1964 ± 28 kg C ha^{-1}) was much lower than that in Y2 (4699 ± 27 kg C ha^{-1}) due to the maize lodging and a lower fertilization rate in Y1 (210 and 250 kg N ha^{-1} in Y1 and Y2, respectively). Thus, the NEP of the wheat–maize field in Y1 (4521 ± 45 kg C ha^{-1}) was only 36% of that in Y2 (7080 ± 48 kg C ha^{-1}, Table 3). Compared with the wheat–maize field, the annual NEP of the cotton field was extremely low (363 and 849 kg C ha^{-1} yr^{-1} in Y1 and Y2, respectively) due to the substantial CO_2 emissions (1568 and 1407 kg C ha^{-1} in Y1 and Y2, respectively) during the long duration of fallow periods (155 and 134 days yr^{-1} in Y1 and Y2, respectively, Fig. 3). The NEP of the cotton field in Y1 (363 ± 31 kg C ha^{-1}) was also slightly lower than that in Y2 (849 ± 34 kg C ha^{-1}) as a result of the different climate and management practices (fertilization rates: 75 and 89 kg N ha^{-1} yr^{-1} in Y1 and Y2, respectively) between the two year-round crop cycles.

The carbon inputs by seeding and fertilization were 69 ± 5 and 73 ± 6 kg C ha^{-1} yr^{-1} in Y1 and Y2, respectively, which were 9%–19% of the NEP in the cotton field. The carbon inputs by seeding and fertilization were 262 ± 15 and 274 ± 16 kg C ha^{-1} yr^{-1} in Y1 and Y2, respectively,

Table 2
Seeding and harvesting information.

Crops	Seeding grain		Crop yield		Grain carbon content		Crop residue				Harvest index		PFP_N	
	kg ha^{-1}		kg ha^{-1}		g C kg^{-1} grain		kg ha^{-1}		kg C ha^{-1}				kg grain kg^{-1} N	
	Y1	Y2	Y1	Y1			Y1	Y2	Y1	Y2	Y1	Y2	Y1	Y2
Wheat	200	200	6116	6365	385	437	8731	8088	3687	3640	0.41	0.44	34	35
	(20)	(20)	(567)	(568)	(15)	(9)	(762)	(790)	(331)	(364)	(0.02)	(0.01)	(3)	(4)
Maize	30	30	6142	6898	429	451	7642	11,547	3367	5075	0.43	0.38	29	28
	(4)	(4)	(674)	(694)	(7)	(5)	(759)	(1031)	(351)	(568)	(0.05)	(0.04)	(4)	(4)
Cotton	66	66	3659	3370	535	563	5444	7215	2495	3120	0.40	0.32	49	38
	(7)	(7)	(493)	(472)	(13)	(3)	(575)	(801)	(182)	(254)	(0.06)	(0.05)	(7)	(5)

Y1 and Y2: 1st and 2nd year-round crop cycles, respectively. PFP_N: the partial factor productivity of applied nitrogen. Values in parentheses indicate standard deviations of four spatial replicates.

which were only 4%–6% of the NEP in the wheat–maize field. The total carbon inputs by NEP, seeding and fertilization were 432 ± 31 and 4783 ± 48 kg C ha^{-1} yr^{-1} in Y1 and 922 ± 35 and 7354 ± 50 kg C ha^{-1} yr^{-1} in Y2 in the cotton and wheat–maize fields, respectively. The carbon inputs in Y1 were lower than those in Y2 because of the lower NEP in Y1 compared with Y2, especially in the wheat–maize field (Table 3).

The carbon outputs by harvested seed cotton were similar in Y1 (1959 ± 277 kg C ha^{-1} yr^{-1}) and Y2 (1896 ± 266 kg C ha^{-1} yr^{-1}), whereas the carbon outputs by harvested wheat and maize grains were much lower in Y1 (4985 ± 375 kg C ha^{-1} yr^{-1}) than those in Y2 (5893 ± 405 kg C ha^{-1} yr^{-1}) as a result of the low grain yields and carbon contents in Y1. The NECBs were finally calculated to be −1527 ± 279 and −202 ± 378 kg C ha^{-1} yr^{-1} in Y1 and −974 ± 268 and 1461 ± 408 kg C ha^{-1} yr^{-1} in Y2 in the cotton and wheat–maize fields, respectively. The cotton field consistently functioned as a strong carbon source to the atmosphere, whereas the wheat–maize field was near net carbon neutral in Y1 and a notable carbon sink in Y2 (Table 3).

3.3. GHGBs

The cotton (−3.1 ± 0.1 and −2.3 ± 0.1 kg CH_4 ha^{-1} yr^{-1} in Y1 and Y2, respectively) and wheat–maize fields (−2.4 ± 0.1 and −1.9 ± 0.1 kg CH_4 ha^{-1} yr^{-1} in Y1 and Y2, respectively) were notable atmospheric CH_4 sinks (Table 4). The CH_4 uptake presented similar seasonal variations and high spatial variabilities in both fields (Fig. 2). The seasonal variations were mainly dependent on temperature fluctuations, as indicated by the significant exponential relationships between soil temperatures and fluxes ($p < 0.01$, Fig. 4). In this study, the Q_{10} was defined as the factor by which CH_4 uptake was multiplied when soil temperature increases by 10 °C, which was calculated to be 1.58 and 1.51 in the cotton and wheat–maize fields, respectively. Substantial CH_4 uptake was observed from May to July, which contributed to 36%–39% and 39%–45% of the annual uptake in the cotton and wheat–maize field, respectively (Fig. 3). During the remaining periods, the CH_4 uptake was relatively weak, and most of the fluxes were near the detection limits of the measuring system (Fig. 2). Although soil WFPS was not significantly correlated with CH_4 fluxes, the very high CH_4 uptake (> 1 mg CH_4 m^{-2} d^{-1}) was mostly accompanied by moderate soil moistures (WFPS: 20%–60%, Fig. 4). Furthermore, the annual CH_4 uptakes and mean WFPS presented opposite inter-annual variations in both fields, which might indicate that precipitation and soil moisture were the determinant factors of inter-annual variations of cumulative CH_4 uptake (Tables 1 and 4).

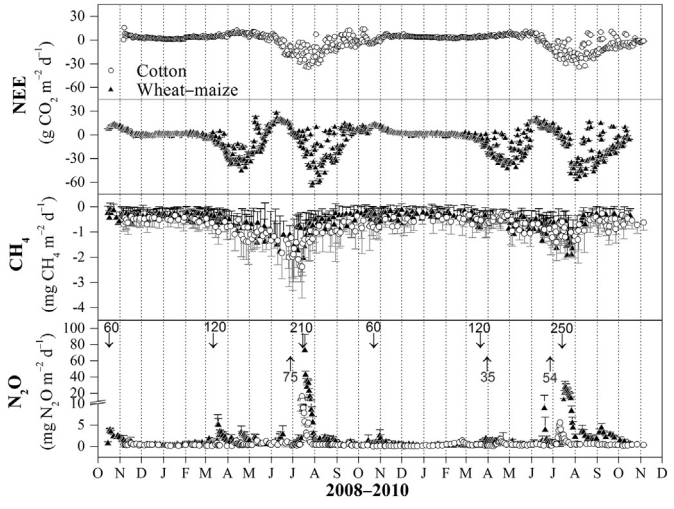

Fig. 2. Daily net ecosystem exchange of CO_2 (NEE) and CH_4 and N_2O fluxes in the cotton and wheat–maize fields. The arrows and numbers indicate the fertilization dates and rates (unit: kg N ha^{-1}) in the cotton (up arrow) and wheat–maize fields (down arrow). The error lines indicate the uncertainties of daily fluxes in the cotton (grey) and wheat–maize fields (black).

The annual cumulative N_2O emissions from the cotton field were 2.4 ± 0.1 and 1.8 ± 0.1 kg N_2O ha^{-1} yr^{-1} in Y1 and Y2, respectively, of which 70%–80% occurred in the cotton growing seasons (April to November). The annual cumulative N_2O emissions from the wheat–maize field were 7.0 ± 0.2 and 5.5 ± 0.2 kg N_2O ha^{-1} yr^{-1} in Y1 and Y2, respectively, of which 67%–80% concentrated on the maize seasons (Table 4 and Fig. 3). Both fields are strong N_2O sources to the atmosphere. Fertilization observably influenced the seasonal variations of N_2O fluxes in the cotton (0.06 to 16.0 mg N_2O m^{-2} d^{-1}) and wheat–maize fields (0.03 to 72.6 mg N_2O m^{-2} d^{-1}, Fig. 2). The high fertilization rates (54–75 and 210–250 kg N ha^{-1} for cotton and maize) and appropriate soil temperatures (20–30 °C) and moistures (WFPS: 30%–60%) in July stimulated N_2O emissions (up to 16.0 and 72.6 mg N_2O m^{-2} d^{-1}) from the cotton and wheat–maize fields (Figs. 2 and 4). The peak N_2O emissions continued for approximately 10–18 days after the fertilization and irrigation in July, which contributed to 18%–39% and 45%–51% of the annual cumulative emissions from the cotton and wheat–maize fields, respectively.

The warming effects of N_2O emissions (648 ± 17 and 486 ± 15 kg $CO_{2\text{-eq}}$ ha^{-1} in Y1 and Y2, respectively) were approximately compensated by the cooling effects of CH_4 uptake (−629 ± 14 and −467 ± 11 kg $CO_{2\text{-eq}}$ ha^{-1} in Y1 and Y2, respectively, with a 100-year time horizon) in the cotton field. Therefore, the NECBs were the determining factors for the values of GHGBs in the cotton field. The cotton field always behaved as a strong GHG source (5618 ± 1022 and 3591 ± 984 kg $CO_{2\text{-eq}}$ ha^{-1} in Y1 and Y2, respectively) because of the negative NECBs in both year-round crop cycles. The cooling effects of CH_4 uptake (−487 ± 14 and −386 ± 12 kg $CO_{2\text{-eq}}$ ha^{-1} in Y1 and Y2, respectively) only offset about 1/4 of the warming effects of N_2O emissions (1890 ± 65 and 1485 ± 53 kg $CO_{2\text{-eq}}$ ha^{-1} in Y1 and Y2, respectively, with a 100-year time horizon) in the wheat–maize field. The wheat–maize field was near net carbon neutral in Y1 (−202 ± 378 kg C ha^{-1} yr^{-1}) and

Table 3
Estimates of net ecosystem carbon budgets (NECBs, unit: kg C ha^{-1}).

Period	C_{inputs}						$C_{exports}$		NECBs	
	NEP		F_{seed}		F_{fert}		F_{harv}			
	Y1	Y2	Y1	Y2	Y1	Y2	Y1	Y2	Y1	Y2
Wheat season	2557	2381	82	77	77	77	2353	2781	363	−246
	(36)	(39)	(9)	(8)	(8)	(8)	(236)	(254)	(239)	(257)
Maize season	1964	4699	13	13	90	107	2632	3112	−565	1707
	(28)	(27)	(2)	(2)	(9)	(11)	(292)	(315)	(293)	(316)
Annual wheat–maize	4521	7080	95	90	167	184	4985	5893	−202	1461
	(45)	(48)	(9)	(8)	(12)	(14)	(375)	(405)	(378)	(408)
Annual cotton	363	849	37	35	32	38	1959	1896	−1527	−974
	(31)	(34)	(4)	(4)	(3)	(4)	(277)	(266)	(279)	(268)

Y1 and Y2: 1st and 2nd year-round crop cycles, respectively. C_{inputs} and $C_{exports}$: the carbon inputs (net ecosystem production and non-CO_2 carbon inputs by seeding and fertilization) and exports (harvest), respectively. NEP: net ecosystem production (approximately equal to the cumulative net ecosystem exchange of CO_2). F_{seed}, F_{fert}, and F_{harv}: the non-CO_2 carbon exchanges by seeding, fertilization, and harvest, respectively. Values in parentheses indicate the uncertainties as described in the uncertainty analysis section.

a strong carbon sink in Y2 (1461 ± 408 kg C ha^{-1} yr^{-1}). Therefore, the double cropping system functioned as a GHG source (2144 ± 1389 kg $CO_{2\text{-eq}}$ ha^{-1}) in Y1 as a result of the net carbon neutral and high N_2O emissions and served as a notable GHG sink (−4257 ± 1496 kg $CO_{2\text{-eq}}$ ha^{-1}) in Y2 because of the high NEP and NECBs (Table 4).

4. Discussion

4.1. Variabilities of the NECBs and GHGBs in fiber and cereal cropping systems

Ceschia et al. (2010) evaluated the NECBs for representative European croplands by considering the NEE, and inputs (organic fertilization and seeds) and outputs of non-CO_2 carbon (harvest). The estimated NECBs fluctuated between −2580 and 6450 kg C ha^{-1} yr^{-1} due to the differences in crop species, climatic conditions, and management practices. The GHGBs were also evaluated by considering the NECBs, N_2O emissions from fertilizer and crop residue applications, and carbon emissions from the fuel and electricity consumption of field operations, agrochemical production, and manufacturing of agricultural machinery. The estimated GHGBs ranged from −6673 to 32,267 kg CO_2-eq ha^{-1} yr^{-1}, using the concept of GWPs with a 100-year time horizon (Ceschia et al., 2010). The NECBs and GHGBs in the present cotton and wheat–maize fields are within these ranges. However, it should be mentioned that the carbon emissions from mechanical operations, agrochemical production, and manufacturing of agricultural machinery were not considered in the present study. Furthermore, the SGCP of CH_4 is 203 when fluxes are into ecosystems, and the SGWP of N_2O is 270 when fluxes are out of ecosystems, with a 100-year time horizon (Neubauer and Megonigal, 2015). The GWPs of CH_4 and N_2O are 34 and 298, respectively, with a 100-year time horizon (Myhre et al., 2013). The application of SGWP and SGCP in the present study particularly enhanced the cooling effects of CH_4 uptake in the estimation of GHGBs compared with the commonly applied concept of GWPs in other studies (Ceschia et al., 2010; Jia et al., 2012; Huang et al., 2013; Ma et al., 2013; Lv et al., 2014).

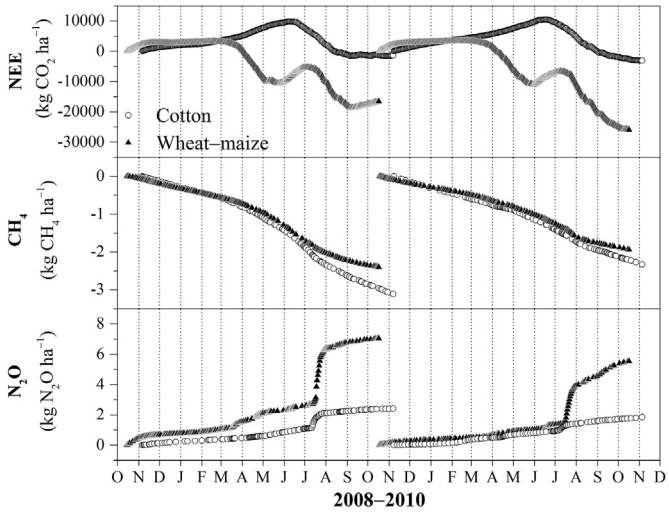

Fig. 3. Cumulative net ecosystem exchange of CO_2 (NEE), CH_4 and N_2O fluxes in the cotton and wheat–maize fields.

Huang et al. (2013) measured N_2O fluxes over two years (2011−2013) and the differences of SOC densities over a 6-year period (in 2006 and 2012) in a winter wheat–summer maize rotational cropping system in the North China Plain. The topsoil (0–20 cm) organic carbon sequestration rates and N_2O emissions under the conventional management practices (fertilization rate: 560 kg N ha^{-1} yr^{-1} and straw amendment) were 1441 kg C ha^{-1} yr^{-1} and 6.8–7.0 kg N_2O ha^{-1} yr^{-1}, which were similar to or slightly higher than the NECBs and N_2O emissions in the wheat–maize field of the present study (NECBs: 1461 ± 408 kg C ha^{-1} yr^{-1} in Y2; N_2O emissions: 7.0 and 5.5 kg N_2O ha^{-1} yr^{-1} in Y1 and Y2, respectively). The GHGBs by considering SOC sequestration and N_2O emissions were estimated to be approximately −3200 kg $CO_{2\text{-eq}}$ ha^{-1} yr^{-1} using the concept of GWPs and therefore, the wheat–maize rational cropping system in the North China Plain also served as an integrated GHG sink. The studies in the North China Plain (Huang et al., 2013) and the Fen-wei Plain (this study) together proved that the typical wheat–maize rational cropping systems with high application rates of irrigation water (210–434 mm yr^{-1}) and chemical fertilizer (390–560 kg N ha^{-1} yr^{-1}) in China could be notable GHG sinks as a result of high net carbon sequestration under the management mode of straw amendment.

The increasing incidences of extreme weather under the background of climate change could weaken the function of the wheat–maize rotational cropping systems as carbon and GHG sinks. The NEP during the maize season in Y1 was only 42% of that in Y2 in the present wheat–maize field. The slightly lower irrigation amount (128 vs. 154 mm) and fertilization rate (210 vs. 250 kg N ha^{-1}) partly contributed to the lower NEP in Y1 compared with Y2. Furthermore, the strong wind on July 9, 2009 damaged the maize plants and caused maize lodging in which maize stems were bent over the ground. The stems and leaves turned yellow and started decaying in early September, which greatly shortened the duration of net CO_2 assimilation in Y1 (July to early September) compared with Y2 (July to mid-October). The maize lodging caused by wind damage substantially contributed to the lowered NEP and therefore the wheat–maize field was near carbon neutral rather than a carbon sink in Y1. Ceschia et al. (2010) also observed that a hail event caused damage to the plants and reduced the net carbon

Table 4
Estimates of greenhouse gas budgets (GHGBs) with a 100-year time horizon.

Period	NECBs				F_{CH4}				F_{N2O}				GHGBs	
	kg C ha^{-1}		kg CO_2-eq ha^{-1}		kg CH_4 ha^{-1}		kg CO_2-eq ha^{-1}		kg N_2O ha^{-1}		kg CO_2-eq ha^{-1}		kg CO_2-eq ha^{-1}	
	Y1	Y2	Y1	Y2	Y1	Y2	Y1	Y2	Y1	Y2	Y1	Y2	Y1	Y2
Wheat season	363	−246	1329	−902	−1.3	−1.1	−264	−223	2.3	1.1	621	297	−972	976
	(239)	(257)	(877)	(943)	(0.05)	(0.04)	(10)	(8)	(0.1)	(0.1)	(19)	(14)	(877)	(943)
Maize season	−565	1707	−2071	6258	−1.1	−0.8	−223	−162	4.7	4.4	1269	1188	3116	−5233
	(293)	(316)	(1076)	(1160)	(0.05)	(0.04)	(10)	(8)	(0.2)	(0.2)	(62)	(52)	(1078)	(1161)
Annual wheat–maize	−202	1461	−741	5356	−2.4	−1.9	−487	−386	7.0	5.5	1890	1485	2144	−4257
	(378)	(408)	(1388)	(1495)	(0.1)	(0.1)	(14)	(12)	(0.2)	(0.2)	(65)	(53)	(1389)	(1496)
Annual cotton	−1527	−974	−5599	−3572	−3.1	−2.3	−629	−467	2.4	1.8	648	486	5618	3591
	(279)	(268)	(1022)	(984)	(0.1)	(0.1)	(14)	(11)	(0.1)	(0.1)	(17)	(15)	(1022)	(984)

Y1 and Y2: 1st and 2nd year-round crop cycles, respectively. NECBs: net ecosystem carbon budgets. F_{CH4} and F_{N2O}: the cumulative CH_4 and N_2O fluxes, respectively. Values in parentheses indicate the uncertainties as described in the uncertainty analysis section.

sequestration in European maize and potato fields. Joo et al. (2016) found that a severe drought event could lower the NEP of a perennial grass in the following year. Thus, extreme weather, such as wind damage and hail and drought events, greatly influence the NEP and increase the variabilities of NECBs and GHGBs in agroecosystems. The integrated measurement of NEE, non-CO_2 carbon exchange, CH_4 and N_2O fluxes is an exclusive method to characterize the short-term (year by year) effects of extreme weather on the NECBs and GHGBs.

Cotton is the world's most important fiber crop but the evaluation of NECBs and GHGBs remain limited for cotton on a global scale. Lv et al. (2014) estimated the NECBs by the changes of topsoil (0–20 cm) organic carbon densities over a 22-year period (in 1990 and 2012) and the GHGBs by adding CH_4 and N_2O fluxes to the NECBs, based on the concept of GWPs with a 100-year time horizon, in a cotton cropping system in Xinjiang Uygur Autonomous Region, northwest China. The annual CH_4 uptake and N_2O emissions in the cotton cropping system in the typical oasis region of northwest China were 4.9 kg CH_4 ha^{-1} yr^{-1} and 3.1 kg N_2O ha^{-1} yr^{-1}, which were higher than the values of the cotton cropping system in the present study (2.3–3.1 kg CH_4 ha^{-1} yr^{-1} and 1.8–2.4 kg N_2O ha^{-1} yr^{-1}). We expect that the extremely arid climate (precipitation: 310 mm yr^{-1} vs. 592–620 mm yr^{-1}) and high fertilization rates (240 N ha^{-1} yr^{-1} vs. 75–89 N ha^{-1} yr^{-1}) were beneficial to CH_4 uptake and N_2O emissions in the cotton cropping system of northwest China compared with the cotton cropping system of the Fen-wei Plain. The average SOC sequestration rate was approximately 20 kg C ha^{-1} yr^{-1} during the 22-year period and therefore, the cotton cropping system in northwest China functioned as net carbon neutral. Due to the high CO_2 emissions during the long fallow periods (134–155 days yr^{-1}), the present cotton cropping system in the Fen-wei Plain persistently served as a notable carbon source (−974 to −1527 kg C ha^{-1} yr^{-1}). The GHGBs in the cotton cropping system of northwest China (871 kg CO_2-eq ha^{-1} yr^{-1}) were also much lower than those in the cotton cropping system of the present study (3591 to 5618 kg CO_2-eq ha^{-1} yr^{-1}). Thus, the diversity in climates and management practices resulted in considerable inter-annual and spatial differences in the NECBs and GHGBs of fiber and cereal cropping systems and the radiative forcing effects of fiber and cereal production on climate change.

Inorganic sources and sinks of CO_2 (weathering reactions, precipitation, dissolution of carbonates, synthetic fertilizer, and atmosphere–water equilibrations) are negligible terms in estimates of NECBs in croplands. The NECBs primarily represent the variations of organic carbon in agroecosystems (plant, litter, and soil). Except for the harvested seed cotton, wheat and maize grains, all crop residues were amended in soils in the present study. Therefore, the variations of NECBs mainly influenced SOC contents in the cotton and wheat-maize fields. The

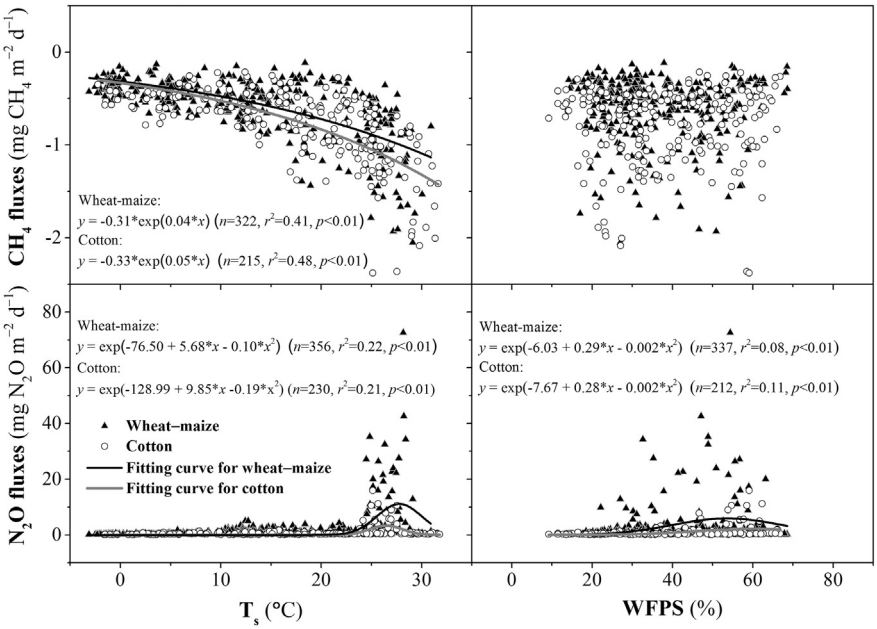
CH4 fluxes (mg CH4 m-2 d-1)
N2O fluxes (mg N2O m-2 d-1)
Wheat-maize:
y = -0.31*exp(0.04*x) (n=322, r2=0.41, p<0.01)
Cotton:
y = -0.33*exp(0.05*x) (n=215, r2=0.48, p<0.01)
Wheat-maize:
y = exp(-76.50 + 5.68*x - 0.10*x2) (n=356, r2=0.22, p<0.01)
Cotton:
y = exp(-128.99 + 9.85*x -0.19*x2) (n=230, r2=0.21, p<0.01)
Wheat-maize:
y = exp(-6.03 + 0.29*x - 0.002*x2) (n=337, r2=0.08, p<0.01)
Cotton:
y = exp(-7.67 + 0.28*x - 0.002*x2) (n=212, r2=0.11, p<0.01)
Wheat–maize
Cotton
Fitting curve for wheat–maize
Fitting curve for cotton
Ts (°C)
WFPS (%)

Fig. 4. Correlations between environmental factors (T_s: soil temperature, and WFPS: soil water-filled pore space) and chamber (CH_4 and N_2O) fluxes.

positive NECBs indicate an increase in SOC contents, which has a positive radiative forcing effect. However, soil organic matter consists of dissolved organic matter, particulate organic matter, humus, and resistant organic matter. The four fractions of soil organic matter vary widely in size, composition, and turnover times. The carbon in fresh residues, living organisms, dissolved organic matter, and particulate organic matter can leave the ecosystem in short terms (1–5 yrs). Only the carbon in humus and resistant organic matter is able to mitigate climate change over long terms (decades to centuries). Although the measured SOC contains both recalcitrant and labile soil carbon, the measurement of SOC density variations over years and decades somehow characterizes the averaged climate impacts during the measuring period (years to decades, Robertson et al., 2000; Shang et al., 2011; Huang et al., 2013; Zhang et al., 2016). The estimate of NECBs indicates the short-term (year by year) net carbon accumulation and loss rates in the ecosystem, whereas the measurement of SOC density variations represents the long-term (years to decades) organic carbon accumulation and loss rates in the soil.

4.2. Advantages of the rotation system between fiber and cereal crops

Longer crop growing days resulted in a longer period of net CO_2 assimilation in the double cropping system of wheat–maize rotation compared with the single cropping system of cotton (346 vs. 247 days during the two year-round crop cycles). The high application rates of irrigation water (408–434 mm yr^{-1} vs. 144–181 mm yr^{-1}) and chemical fertilizer (390–430 kg N ha^{-1} yr^{-1} vs. 75–89 N ha^{-1} yr^{-1}) enhanced the net CO_2 assimilation rates (average of negative NEE: -18.4 g CO_2 m^{-2} d^{-1} vs. -10.5 g CO_2 m^{-2} d^{-1}) in the wheat–maize rotational cropping system compared with the cotton cropping system. Thus, the double cropping system of wheat–maize rotation had very high annual NEP when wind damage did not occur (7080 ± 64 kg C ha^{-1} yr^{-1}). The high annual NEP and the management practices of crop residue amendment and low harvest indices (< 0.44) resulted in the high NECBs in the wheat–maize rotational cropping system. Although the high irrigation water and chemical fertilizer inputs stimulated N_2O emissions and weakened CH_4 uptake, the integrated evaluation of GHGBs showed that the double cropping system still functioned as a notable GHG sink because of the substantial NEP and net carbon sequestration. The probability of extreme weather occurrence is increasing and extreme weather may lower the NEP and NECBs, but such severe wind damage in Y1 is still rare. Thus, this study suggests that the double cropping system of wheat-maize rotation generally exceeds the single cropping system of cotton regarding the NEP, NECBs and GHGBs.

The rotation between fiber (cotton) and cereal (wheat, maize, or sorghum) cropping systems in an interval of 2–3 years is a traditional management practice to avoid the negative effects of monoculture on crop yields in the experimental region before 2004. The evaluation of NECBs in the present study demonstrated that the net carbon losses during the cotton planting cycle (NECBs: -974 to -1527 kg C ha^{-1} yr^{-1}, planting cycle: 2–3 years) could be largely compensated by the net carbon sequestration during the wheat–maize planting cycle (NECBs: 1461 kg C ha^{-1} yr^{-1}, planting cycle: 2–3 years) under the traditional rotation system. However, the cotton planting cycles have been increased to 5–6 years, whereas the wheat–maize planting cycles are reduced to 0–1 years in the most recent decade to maximize economic benefits from cotton cultivation. Current cotton production is extremely dependent on the application of agrochemicals (e.g., weekly applications of pesticide from mid-May to mid-August in the present cotton field), and lead to great carbon losses and positive radiative forcing effects. In contrast, the wheat–maize rotational cropping system has notable carbon sequestration and negative radiative forcing effects with much lower application rates of agrochemicals (e.g., once per year for pesticide application). Thus, the traditional rotation between fiber and cereal cropping systems should be restored to stabilize soil carbon storage, reduce reliance on agrochemical applications, and alleviate the radiative forcing effects of cotton production on climate change.

The nitrogen use efficiencies in the present cotton and wheat–maize fields (PFP_N: 38–49 and 31 kg grain kg^{-1} N) were much lower than the global mean values (40–70 kg grain kg^{-1} N, Dobermann, 2005). The heavy reliance of fiber and cereal production on the overuse of irrigation water and chemical fertilizers cannot be sustained due to the rapid fall of groundwater level and the environmental pollution caused by nitrate leaching and ammonia volatilization in the Fen-wei Plain. Furthermore, the crop residues are returned to the soil in the present cotton and wheat–maize fields. If the crop residues are removed as silage or biomass energy in future, the cotton and wheat–maize fields will definitely become extremely strong sources of carbon (NECBs: -4022 to -4094 kg C ha^{-1} yr^{-1} and -7254 to -7256 kg C ha^{-1} yr^{-1} in the cotton and wheat–maize field, respectively) and GHGs (GHGBs: 14766 to 15,031 kg $CO_{2\text{-eq}}$ ha^{-1} yr^{-1} and 27,699 to 28,009 kg $CO_{2\text{-eq}}$ ha^{-1} yr^{-1}). Thus, the improvement of water and nitrogen use efficiencies, the continuous popularization of crop residue amendment, and the recovery of traditional rotation between fiber and cereal cropping systems all are vital for the sustainability of fiber and cereal production in China.

5. Conclusions

It is generally accepted that high application rates of irrigation water and chemical fertilizer stimulate GHG emissions from agroecosystems. However, the evaluation of NECBs and GHGBs showed that the wheat–maize rotational cropping system with extremely high water and fertilizer inputs could be a notable carbon and GHG sink, whereas the cotton cropping system with low water and fertilizer inputs was a strong carbon and GHG source. The cooling effects of CH_4 uptake was exactly offset by the warming effects of N_2O emissions in the cotton cropping system. The cotton cropping system consistently functioned as a strong carbon and GHG source because of the substantial CO_2 emissions during the long bare fallow period. The longer crop growing periods and the higher irrigation water and chemical fertilizer inputs greatly increased the NEP in the wheat–maize rotational cropping system compared with the cotton cropping system. The high NEP alongside the management mode of crop residue amendment led to high net carbon sequestration in the wheat–maize rotational cropping system. Although the high application rates of irrigation water and chemical fertilizer stimulated N_2O emissions, the wheat–maize rotational cropping system still behaved as an integrated GHG sink because of the high NEP and NECBs. Incidental wind damage could heavily lower the NEP and turn the wheat–maize rotational cropping system into a GHG source. However, the double cropping system of cereal crops commonly exceeded the single cropping system of the fiber crop in terms of the NEP, carbon sequestration, and integrated climate effects of GHG exchanges. Thus, the traditional rotation between double (cereal) and single (fiber) cropping systems should be restored to maintain soil carbon storage, reduce reliance on agrochemical applications, and mitigate the radiative forcing effects of fiber production on climate change. The large inter-annual and spatial variabilities in the NECBs and GHGBs indicate that the regionalization of net biome productivity (extrapolation of NECBs to larger spatial scales) and GHGBs remains challenging.

Acknowledgements

This study was financially supported by the Ministry of Science and Technology of the People's Republic of China (2016YFA0602303) and the National Natural Science Foundation of China (41761144054).

References

Aubinet, M., Moureaux, C., Bodson, B., Dufranne, D., Heinesch, B., Suleau, M., Vancutsem, F., Vilret, A., 2009. Carbon sequestration by a crop over a 4-year sugar beet/winter wheat/seed potato/winter wheat rotation cycle. Agric. For. Meteorol. 149, 407–418.

Béziat, P., Ceschia, E., Dedieu, G., 2009. Carbon balance of a three crop succession over two cropland sites in South West France. Agric. For. Meteorol. 149, 1628–1645.
Bhattacharyya, P., Neogi, S., Roy, K.S., Dash, P.K., Tripathi, R., Rao, K.S., 2013. Net ecosystem CO_2 exchange and carbon cycling in tropical lowland flooded rice ecosystem. Nutr. Cycl. Agroecosyst. 95, 133–144.
Burba, G.G., McDermitt, D.K., Grelle, A., Anderson, D.J., Xu, L., 2008. Addressing the influence of instrument surface heat exchange on the measurements of CO_2 flux from open-path gas analyzers. Glob. Chang. Biol. 14, 1854–1876.
Ceschia, E., Béziat, P., Dejoux, J.F., Aubinet, M., Bernhofer, C., Bodson, B., Buchmann, N., Carrara, A., Cellier, P., Di Tommasi, P., Elbers, J.A., Eugster, W., Grünwald, T., Jacobs, C.M.J., Jans, W.W.P., Jones, M., Kutsch, W., Lanigan, G., Magliulo, E., Marloie, O., Moors, E.J., Moureaux, C., Olioso, A., Osborne, B., Sanz, M.J., Saunders, M., Smith, P., Soegaard, H., Wattenbach, M., 2010. Management effects on net ecosystem carbon and GHG budgets at European crop sites. Agric. Ecosyst. Environ. 139, 363–383.
Chapin, F.S., Woodwell, G.M., Randerson, J.T., Rastetter, E.B., Lovett, G.M., Baldocchi, D.D., Clark, D.A., Harmon, M.E., Schimel, D.S., Valentini, R., Wirth, C., Aber, J.D., Cole, J.J., Goulden, M.L., Harden, J.W., Heimann, M., Howarth, R.W., Matson, P.A., McGuire, A.D., Melillo, J.M., Mooney, H.A., Neff, J.C., Houghton, R.A., Pace, M.L., Ryan, M.G., Running, S.W., Sala, O.E., Schlesinger, W.H., Schulze, E.D., 2006. Reconciling carbon-cycle concepts, terminology, and methods. Ecosystems 9, 1041–1050.
China statistical yearbook, 2017. Agriculture. Compiled by National Bureau of Statistics of China. China Statistics Press, Beijing, China.
Dobermann, A.R., 2005. Nitrogen Use Efficiency - State of the Art. Agronomy & Horticulture. Faculty Publications paper 316. http://digitalcommons.unl.edu/agronomyfacpub/316.
Fan, S.-M., Wofsy, S.C., Bakwin, P.S., Jacob, D.J., 1990. Atmosphere-biosphere exchange of CO_2 and O_3 in the Central Amazon Forest. J. Geophys. Res. 95 (D10), 16,851–16,864.
Finkelstein, P.L., Sims, P.F., 2001. Sampling error in eddy correlation flux measurements. J. Geophys. Res. 106 (D4), 3503–3509.
Foken, T., Wichura, B., 1996. Tools for quality assessment of surface-based flux measurements. Agric. For. Meteorol. 78, 83–105.
Foley, J.A., Ramankutty, N., Brauman, K.A., Cassidy, E.S., Gerber, J.S., Johnston, M., Mueller, N.D., O'Connell, C., Ray, D.K., West, P.C., Balzer, C., Bennett, E.M., Carpenter, S.R., Hill, J., Monfreda, C., Polasky, S., Rockstrom, J., Sheehan, J., Siebert, S., Tilman, D., Zaks, D.P., 2011. Solutions for a cultivated planet. Nature 478, 337–342.
Göckede, M., Markkanen, T., Charlotte, B.H., Foken, T., 2006. Update of a footprint-based approach for the characterisation of complex measurement sites. Bound.-Layer Meteorol. 118, 635–655.
Huang, T., Gao, B., Christie, P., Ju, X., 2013. Net global warming potential and greenhouse gas intensity in a double-cropping cereal rotation as affected by nitrogen and straw management. Biogeosciences 10, 7897–7911.
Jia, J.X., Ma, Y.C., Xiong, Z.Q., 2012. Net ecosystem carbon budget, net global warming potential and greenhouse gas intensity in intensive vegetable ecosystems in China. Agric. Ecosyst. Environ. 150, 27–37.
Joo, E., Hussain, M.Z., Zeri, M., Masters, M.D., Miller, J.N., Gomez-Casanovas, N., Delucia, E.H., Bernacchi, C.J., 2016. The influence of drought and heat stress on long-term carbon fluxes of bioenergy crops grown in the Midwestern USA. Plant Cell Environ. 39, 1928–1940.
Kljun, N., Calanca, P., Rotach, M.W., Schmid, H.P., 2004. A simple parameterisation for flux footprint predictions. Bound.-Layer Meteorol. 112, 503–523.
Kutsch, W.L., Aubinet, M., Buchmann, N., Smith, P., Osborne, B., Eugster, W., Wattenbach, M., Schrumpf, M., Schulze, E.D., Tomelleri, E., Ceschia, E., Bernhofer, C., Béziat, P., Carrara, A., Di Tommasi, P., Grünwald, T., Jones, M., Magliulo, V., Marloie, O., Moureaux, C., Olioso, A., Sanz, M.J., Saunders, M., Søgaard, H., Ziegler, W., 2010. The net biome production of full crop rotations in Europe. Agric. Ecosyst. Environ. 139, 336–345.
LI-COR Biosciences, 2017. Eddy Covariance Processing Software (Version 6.2.1) [Software]. Available at. www.licor.com/EddyPro.
Liu, C., Zheng, X., Zhou, Z., Han, S., Wang, Y., Wang, K., Liang, W., Li, M., Chen, D., Yang, Z., 2010. Nitrous oxide and nitric oxide emissions from an irrigated cotton field in Northern China. Plant Soil 332, 123–134.
Liu, C., Wang, K., Meng, S., Zheng, X., Zhou, Z., Han, S., Chen, D., Yang, Z., 2011. Effects of irrigation, fertilization and crop straw management on nitrous oxide and nitric oxide emissions from a wheat–maize rotation field in northern China. Agric. Ecosyst. Environ. 140, 226–233.
Liu, C., Wang, K., Zheng, X., 2012. Responses of N_2O and CH_4 fluxes to fertilizer nitrogen addition rates in an irrigated wheat-maize cropping system in northern China. Biogeosciences 9, 839–850.
Liu, C., Wang, K., Zheng, X., 2013. Effects of nitrification inhibitors (DCD and DMPP) on nitrous oxide emission, crop yield and nitrogen uptake in a wheat–maize cropping system. Biogeosciences 10, 2427–2437.
Liu, C., Lu, M., Cui, J., Li, B., Fang, C., 2014. Effects of straw carbon input on carbon dynamics in agricultural soils: a meta-analysis. Glob. Chang. Biol. 20, 1366–1381.
Lv, J., Liu, X., Liu, H., Wang, X., Li, K., Tian, C., Christie, P., 2014. Greenhouse gas intensity and net annual global warming potential of cotton cropping systems in an extremely arid region. Nutr. Cycl. Agroecosyst. 98, 15–26.
Ma, Y.C., Kong, X.W., Yang, B., Zhang, X.L., Yan, X.Y., Yang, J.C., Xiong, Z.Q., 2013. Net global warming potential and greenhouse gas intensity of annual rice–wheat rotations with integrated soil–crop system management. Agric. Ecosyst. Environ. 164, 209–219.
Moncrieff, J.B., Massheder, J.M., de Bruin, H., Ebers, J., Friborg, T., Heusinkveld, B., Kabat, P., Scott, S., Soegaard, H., Verhoef, A., 1997. A system to measure surface fluxes of momentum, sensible heat, water vapor and carbon dioxide. J. Hydrol. 188-189, 589–611.
Moncrieff, J.B., Clement, R., Finnigan, J., Meyers, T., 2004. Averaging, detrending, and filtering of eddy covariance time series. In: Lee, X., Massman, W., Law, B. (Eds.), Handbook of Micrometeorology: A Guide for Surface Flux Measurements. Kluwer Academic Publishers, Dordrecht.
Myhre, G., Shindell, D., Bréon, F.-M., Collins, W., Fuglestvedt, J., Huang, J., Koch, D., Lamarque, J.-F., Lee, D., Mendoza, B., Nakajima, T., Robock, A., Stephens, G., Takemura, T., Zhang, H., 2013. Anthropogenic and natural radiative forcing. In: Stocker, T.F., Qin, D., Plattner, G.-K., Tignor, M., Allen, S.K., Boschung, J., Nauels, A., Xia, Y., Bex, V., Midgley, P.M. (Eds.), Climate Change 2013: The Physical Science Basis. Contribution of Working Group I to the Fifth Assessment Report of the Intergovernmental Panel on Climate Change. Cambridge University Press, Cambridge, United Kingdom and New York, NY, USA.
Neubauer, S.C., Megonigal, J.P., 2015. Moving beyond global warming potentials to quantify the climatic role of ecosystems. Ecosystems 18, 1000–1013.
Robertson, G.P., Paul, E.A., Harwood, R.R., 2000. Greenhouse gases in intensive agriculture: contributions of individual gases to the radiative forcing of the atmosphere. Science 289, 1922–1925.
Scheer, C., Wassmann, R., Kienzler, K., Ibragimov, N., Lamers, J.P.A., Martius, C., 2008. Methane and nitrous oxide fluxes in annual and perennial land-use systems of the irrigated areas in the Aral Sea Basin. Glob. Chang. Biol. 14, 2454–2468.
Shang, Q., Yang, X., Gao, C., Wu, P., Liu, J., Xu, Y., Shen, Q., Zou, J., Guo, S., 2011. Net annual global warming potential and greenhouse gas intensity in Chinese double rice-cropping systems: a 3-year field measurement in long-term fertilizer experiments. Glob. Chang. Biol. 17, 2196–2210.
Smith, P., Lanigan, G., Kutsch, W.L., Buchmann, N., Eugster, W., Aubinet, M., Ceschia, E., Béziat, P., Yeluripati, J.B., Osborne, B., Moors, E.J., Brut, A., Wattenbach, M., Saunders, M., Jones, M., 2010. Measurements necessary for assessing the net ecosystem carbon budget of croplands. Agric. Ecosyst. Environ. 139, 302–315.
Vickers, D., Mahrt, L., 1997. Quality control and flux sampling problems for tower and aircraft data. J. Atmos. Ocean. Technol. 14, 512–526.
Wang, Y., Wang, Y., Ling, H., 2010. A new carrier gas type for accurate measurement of N_2O by GC-ECD. Adv. Atmos. Sci. 27, 1322–1330.
Wang, K., Liu, C., Zheng, X., Pihlatie, M., Li, B., Haapanala, S., Vesala, T., Liu, H., Wang, Y., Liu, G., Hu, F., 2013. Comparison between eddy covariance and automatic chamber techniques for measuring net ecosystem exchange of carbon dioxide in cotton and wheat fields. Biogeosciences 10, 6865–6877.
Webb, E.K., Pearman, G.I., Leuning, R., 1980. Correction of flux measurements for density effects due to heat and water vapour transfer. Quart. J. R. Meteor. Soc. 106, 85–100.
Wilczak, J.M., Oncley, S.P., Stage, S.A., 2001. Sonic anemometer tilt correction algorithms. Bound.-Layer Meteorol. 99, 127–150.
Zhang, X.X., Xu, X., Liu, Y.L., Wang, J.Y., Xiong, Z.Q., 2016. Global warming potential and greenhouse gas intensity in rice agriculture driven by high yields and nitrogen use efficiency. Biogeosciences 13, 2701–2714.